

**A Measurement of $\Lambda_{\overline{MS}}$ from ν_{μ} -Fe Nonsinglet Structure Functions
at the Fermilab Tevatron**

P.Z.Quintas, ¹ W.C.Leung, S.R.Mishra, ² F.Sciulli,

C.Arroyo, K.T.Bachmann, ³ R.E.Blair, ⁴ C.Foudas, ⁵ B.J.King, W.C.Lefmann,

E.Oltman, ⁶ S.A.Rabinowitz, W.G.Seligman, M.H.Shaevitz

Columbia University, New York, NY 10027

F.S.Merritt, M.J.Oreglia, B.A.Schumm⁶

University of Chicago, Chicago, IL 60637

R.H.Bernstein, F. Borcharding, H.E.Fisk, M.J.Lamm,

W.Marsh, K.W.B.Merritt, H.Schellman, ⁷ D.D.Yovanovitch

Fermilab, Batavia, IL 60510

A.Bodek, H.S.Budd, P. de Barbaro, W.K.Sakumoto

University of Rochester, Rochester, NY 14627

P.H.Sandler, W.H.Smith

University of Wisconsin, Madison, WI 53706.

(Nevis Preprint # 1461, Jun.1992)

¹Address after Jan. 1992: Fermilab, Batavia, IL 60510.

²Address after Aug. 1991: Harvard University, Cambridge, MA 02138.

³Present address: N.C.A.R., Boulder, CO 80307.

⁴Present address: Argonne National Laboratory, Argonne, IL 60439.

⁵Present address: University of Wisconsin, Madison, WI 53706.

⁶Present address: Lawrence Berkeley Laboratory, Berkeley, CA 94720.

⁷Present address: Northwestern University, Evanston, IL 60208.

The CCFR collaboration presents a measurement of scaling violations of the non-singlet structure function and a comparison to the predictions of perturbative QCD. The value of $\Lambda_{\overline{MS}}$, from the non-singlet evolution with $Q^2 > 15 \text{ GeV}^2$, is found to be $210 \pm 28(\text{stat.}) \pm 41(\text{syst.}) \text{ MeV}$.

PACS numbers: 13.60Hb; 11.50Li; 12.38Qk; 25.3Fj

Deep inelastic lepton scattering experiments have provided some of the most precise tests of perturbative Quantum Chromodynamics (PQCD). One critical prediction is the Q^2 -dependence of the non-singlet structure function xF_3 ; until now this prediction has not met the test of experimental comparison.[1] PQCD predicts the amount of scaling violation (the Q^2 dependence) from the measured x -dependence of structure functions at fixed Q^2 , and one additional unknown: the strong coupling parameter, α_s , [2]. Since the structure functions are directly measured, the magnitude of the observed scaling violations can be compared to the predictions and simultaneously measure α_s , or $\Lambda_{\overline{MS}}$.

Structure functions evolve in PQCD according to the equations [2]

$$\frac{dF^{NS}(x, Q^2)}{d \ln Q^2} = \frac{\alpha_s(Q^2)}{\pi} \int_x^1 P_{qq}(z, \alpha_s) F^{NS}\left(\frac{x}{z}, Q^2\right) dz \quad (1)$$

$$\frac{dF^S(x, Q^2)}{d \ln Q^2} = \frac{\alpha_s(Q^2)}{\pi} \int_x^1 \left[P_{qq}(z, \alpha_s) F^S\left(\frac{x}{z}, Q^2\right) + P_{qG}(z, \alpha_s) G\left(\frac{x}{z}, Q^2\right) \right] dz \quad (2)$$

where the P_{IJ} are the predicted "splitting functions".[2] The non-singlet evolution depends only on the measured structure functions, the known splitting function, and α_s . The singlet equation is more complicated: its evolution is coupled with that of the gluons. Only the non-singlet evolution can be computed independent of

assumptions about the dependence of the gluon distribution on x and Q^2 . Because $P_{qq}(z)$ passes through zero, the left-hand side of Eq.1 is predicted to pass through zero at about $x = 0.11$, independent of α_s .⁸ A comparison of this prediction with experiment is a fundamental test of PQCD which has not yet been demonstrated.

Neutrino experiments on heavy targets can perform this test with the non-singlet structure function, xF_3 . The high statistics CDHSW data[3] do not agree well with the predicted dependence of the scaling violations on x , although the authors state that the discrepancies are within their systematic errors. Previous CCFR data lacked the statistical power to offer a conclusive test [4].

Currently the most precise deep inelastic tests of PQCD have been obtained from muon scattering data [5] using the singlet structure function, F_2 . These experiments have claimed good agreement with the theory. However, since the evolution of F_2 is coupled to that of the gluon structure function, and since the gluon distributions are not directly measured, corresponding tests of PQCD and determination of $\Lambda_{\overline{MS}}$ necessarily depend on assumptions regarding the x -dependence of the gluon density.

We have reported measurements of F_2 and xF_3 from new data taken in the high energy, high flux Fermilab Tevatron Quadrupole triplet neutrino beamline in Ref.[6] The data for the structure function xF_3 contain sufficiently high statistics and control of systematic uncertainties to address the scaling violation predictions of PQCD, and to permit measurement of $\Lambda_{\overline{MS}}$ with comparable precision to that of

⁸This statement is valid in leading order; in next-to-leading order, all curves parametrized by differing $\Lambda_{\overline{MS}}$ pass through a common point near zero at $x = 0.11$. See Figure 2 of Ref.[6]

recent muon experiments, but without assumptions about gluons.

Measurements of the scaling violations are sensitive to miscalibrations of either the hadron or muon energies (E_{had} or E_{μ}). For example, a 1% miscalibration can cause a 50 MeV mismeasurement of $\Lambda_{\overline{MS}}$, but these errors enter with opposite signs. Thus if both E_{had} and E_{μ} were in error by the same amount, the error in $\Lambda_{\overline{MS}}$ would be small. Therefore, while it is important that the hadron and muon energy calibrations and resolution functions be well known, it is crucial that the energy scales be cross-calibrated to minimize energy uncertainty as a source of error.

The detector was absolutely calibrated using charged particle test beams. A hadron beam, at several different energies, was directed into the target carts at different positions. Each beam particle was momentum analyzed to about 1%. These data were used to calibrate the calorimeter to about 1% and to determine the calorimeter resolution function [7]. In two test runs, separated by three years, the energy calibration constant, normalized to muon response, varied by $\approx 0.3\%$. Normalization of the calorimetric energy to the muon response removes time-dependent calibration changes in the calorimeter. Test beam muons were used to calibrate the toroid spectrometer to $\approx (.5\% - .6\%)$, and to determine the resolution function for muons [7].

The relative calibration of E_{had} to E_{μ} was checked from the ν data by plotting $\frac{\langle E_{vis} \rangle^{DATA}}{\langle E_{vis} \rangle^{MC}}$ ⁹ as a function of $y = E_{had}/E_{vis}$. If the hadron and muon energy scales

⁹ $\langle E_{vis} \rangle^{MC}$ is the visible energy analog to the data from a Monte Carlo simulation of the experiment.

are correct, the ratio will be unity for all y . If not, the two energy scales must be adjusted. To satisfy this constraint, calibration adjustments of $E_\mu \rightarrow E_\mu \times 0.995$ and $E_{had} \rightarrow E_{had} \times 1.016$ were chosen; these adjustments are consistent with the known calibration uncertainty. Figure 1 shows the relative calibration after adjustment of these two parameters. The error on the relative calibration remains ($\approx 0.5\%$) the dominant systematic error in the determination of $\Lambda_{\overline{MS}}$.

We used a modified version of the Duke and Owens program to do a next-to-leading order QCD analysis with target mass correction. [8] Applying cuts $Q^2 > 15$ GeV² to eliminate the non-perturbative region and $x < .7$ to remove the highest x bin (where resolution corrections are sensitive to Fermi motion), best QCD fits to the data were obtained as illustrated in Fig.2 and discussed below.

A good visual representation of structure function evolution compares the magnitude of the Q^2 -dependence of the data in each x -bin with the dependence predicted by the fit. This is shown by plotting the “slopes” ($= \frac{d \ln x F_3}{d \ln Q^2}$) as a function of x . Figure 3 shows our new data along with the curve through the points predicted by the theory. More specifically the values shown in Fig.3 result from power law fits to both data and theory over the Q^2 range of the data. The logarithmic slopes of the data agree well with the QCD prediction throughout the entire x -range. This observation is independent of calibration adjustments within reasonable limits. At low- x values the data agree well with predictions independent of the value of $\Lambda_{\overline{MS}}$. This is the first confirmation of the QCD prediction for scaling violations which is independent of assumptions about the gluon distributions and valid over the entire

x range.

The value of $\Lambda_{\overline{MS}}$ resulting from the fit to xF_3 data was 179 ± 36 MeV, with a χ^2 of 53.5 for 53 degrees of freedom ($\chi^2=53.5/53$). Varying the Q^2 cuts does not significantly change $\Lambda_{\overline{MS}}$; for $Q^2 > 10$ GeV², the best fit gives $\Lambda_{\overline{MS}} = 171 \pm 32$ MeV ($\chi^2=66.4/63$); and for $Q^2 > 5$ GeV², $\Lambda_{\overline{MS}} = 170 \pm 31$ MeV ($\chi^2=83.8/80$).

A more precise determination of $\Lambda_{\overline{MS}}$ from the non-singlet evolution is obtained by substituting F_2 for xF_3 at large values of x . The evolution of F_2 should conform to that of a non-singlet structure function in a region, $x > x_{cut}$, so long as x_{cut} is large enough that the effects of antiquarks, gluons, and the longitudinal structure function are negligible on its Q^2 evolution. A conservative choice for x_{cut} is one beyond which the antiquarks are consistent with zero. Table 1 shows the antiquark content of the nucleon in our highest x -bins. The table also shows the values of $\Lambda_{\overline{MS}}$ from fits where F_2 was substituted for xF_3 in those bins. (We normalized $F_2(x) = xF_3(x)$ for $x > x_{cut}$; an adjustment of $< 3\%$.) For our best value of $\Lambda_{\overline{MS}}$ from non-singlet evolution we choose to substitute F_2 for xF_3 for $x > 0.5$. (The slopes for F_2 in this region are also shown in Figure 3.) This non-singlet fit yields our best value:

$$\Lambda_{\overline{MS}} = 210 \pm 28 \text{ MeV for } Q^2 > 15 \text{ GeV}^2. \quad (3)$$

Varying the x_{cut} from 0.5 to 0.4 does not significantly change $\Lambda_{\overline{MS}}$; the above substitution yields, $\Lambda_{\overline{MS}} = 216 \pm 25$ MeV with good fit. Using $2xF_1$ instead of F_2 in this fit changes $\Lambda_{\overline{MS}}$ by +1 MeV.

We have also done preliminary QCD fits evolving F_2 , and (F_2 & xF_3) simul-

taneously. The quality of these fits is satisfactory; *e.g.* for $\Lambda_{\overline{MS}} = 211$ MeV and $G(x) = A(1-x)^4$ at $Q^0 = 5$ GeV², the PQCD predictions fit F_2 data well as illustrated in Fig.4. Our F_2 data resolves some of the earlier controversies concerning QCD evolution of F_2 in nuclear targets [1]. The values of $\Lambda_{\overline{MS}}$ from F_2 fits are consistent with Eqn.3. It must be pointed out that any value of $\Lambda_{\overline{MS}}$ from such a fit is correlated with the x -dependences of the gluon and antiquark distributions.

The systematic errors on $\Lambda_{\overline{MS}}$ are shown in Table 2. The energy scale error comes from changing both the hadron and muon energies by 1% *in the same direction*. As explained above, the errors from a correlated energy change tend to cancel, resulting in an error of ≈ 10 MeV. The largest error comes from a possible miscalibration of E_{had} with respect to E_μ . The statistics of the relative calibration data allow a 0.6% variation of the two energy scales from the ideal which results in a 48 MeV systematic error (36 MeV for the fit with F_2). The last two errors come from varying the two assumptions of the absolute normalization. The fit with xF_3 alone shows a greater dependence on these assumptions because it is formed from differences of neutrino and antineutrino event sums, while F_2 is derived from the sum of the two. Finally, using radiative correction due to Bardin [9] instead of due to de Rujula [9] gave a shift in $\Lambda_{\overline{MS}}$ of about 5 MeV in preliminary studies.

In summary, we have presented new high energy, high statistics precision measurements of the scaling violations in xF_3 and F_2 . The data provide the first observation of the non-singlet structure function evolution consistent with QCD, and yield $\Lambda_{\overline{MS}} = 210 \pm 28(\text{stat.}) \pm 41(\text{syst.})$ MeV. The measured $\Lambda_{\overline{MS}}$ corresponds

to a strong coupling constant at the Z^0 -pole of, $\alpha_S(M_Z) = 0.111 \pm 0.002 \pm 0.003$; the theoretical uncertainty due to scale dependence in this measurement of α_S is estimated to be about ± 0.0035 [10].

We acknowledge the gracious help of the FNAL staff and the dedicated efforts of many individuals at our home institutions. This research was supported by the National Science Foundation and the Department of Energy.

References

- [1] S.R.Mishra and F.Sciulli, *Annu. Rev. Nucl. Part. Sci.*, **39:259**, 1989.
- [2] G.Altarelli and G.Parisi, *Nucl. Phys.*, **B126:298**, 1977.
- [3] P.Berge *et al.*, *Z. Phys.*, **C49:187**, 1991.
- [4] E.Oltman *et al.*, accepted by *Z. Phys.*, 1991.
- [5] A.C.Benvenuti *et al.*, *Phys. Lett.*, **B195:97**, 1987; A.C.Benvenuti *et al.*, *Phys. Lett.*, **B223:490**, 1989; A.C.Benvenuti *et al.*, *Phys. Lett.*, **B237:592**, 1990.
- [6] S.R.Mishra *et al.*, Nevis Preprint # 1459, submitted to *Phys. Rev. Lett.*, 1991; W.C.Leung *et al.*, Nevis Preprint # 1460, submitted to *Phys. Rev. Lett.*, 1991.
- [7] Calorimeter: W.K.Sakumoto *et al.*, *Nucl. Inst. Meth.*, **A294:179**, 1990; Spectrometer: B.J.King *et al.*, *Nucl. Inst. Meth.*, **A302:254**, 1991.
- [8] A.De Veto *et al.*, *Phys. Rev.*, **D27:508**, 1983.
- [9] D.Yu.Bardin *et al.*, *JINR-E2-86-260* (1986); A.De Rújula *et al.*, *Nucl. Phys.*, **B154:394**, 1979.
- [10] A.D.Martin *et al.*, *Phys.Lett.*, **B266:173**, 1991.

Table 1: Antiquarks and Substitution Fits: Fraction of $\bar{q}(x)$ with respect to $x\text{F}_3$, and the extracted $\Lambda_{\overline{MS}}$ (in MeV) from non-singlet fits, with $Q^2 > 15 \text{ GeV}^2$, are shown.

x -BIN	$x\bar{q}(x)/x\text{F}_3(x)$	$\Lambda_{\overline{MS}}$
no substitution		179 ± 36
0.65	$-0.3 \pm 0.7\%$	218 ± 33
0.55	$1.2 \pm 1.0\%$	210 ± 28
0.45	$3.0 \pm 0.7\%$	216 ± 25

Table 2: Systematic Errors in $\Lambda_{\overline{MS}}$ Measurement: The errors on $\Lambda_{\overline{MS}}$ are in MeV. The last column presents non-singlet fits with $x\text{F}_3$ in the range $x \leq 0.50$ and F_2 in the range $0.50 < x \leq 0.70$.

ERROR	$x\text{F}_3$ alone	$x\text{F}_3 + \text{F}_2$
Energy Scale	± 9	± 19
Rel. Calibr.	± 48	± 36
$\Delta\sigma^{\nu N}$	± 11	± 6
$\Delta\sigma^{\bar{\nu}N}/\sigma^{\nu N}$	± 20	± 2
Total Systematic	± 54	± 41

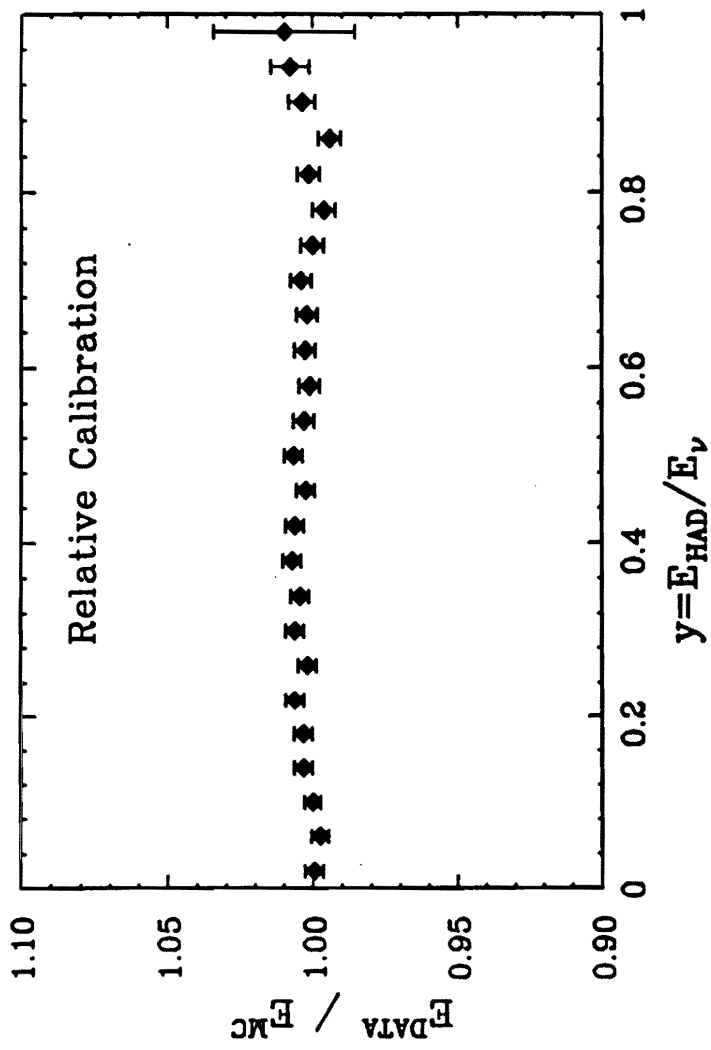
Figure Captions

Figure 1: The relative calibration after the adjustment. We plot E_ν^{DATA}/E_ν^{MC} as a function of y . Adjustments of $E_\mu \rightarrow E_\mu \times 0.995$ and $E_{had} \rightarrow E_{had} \times 1.016$ were made to make the calibration unity for all y .

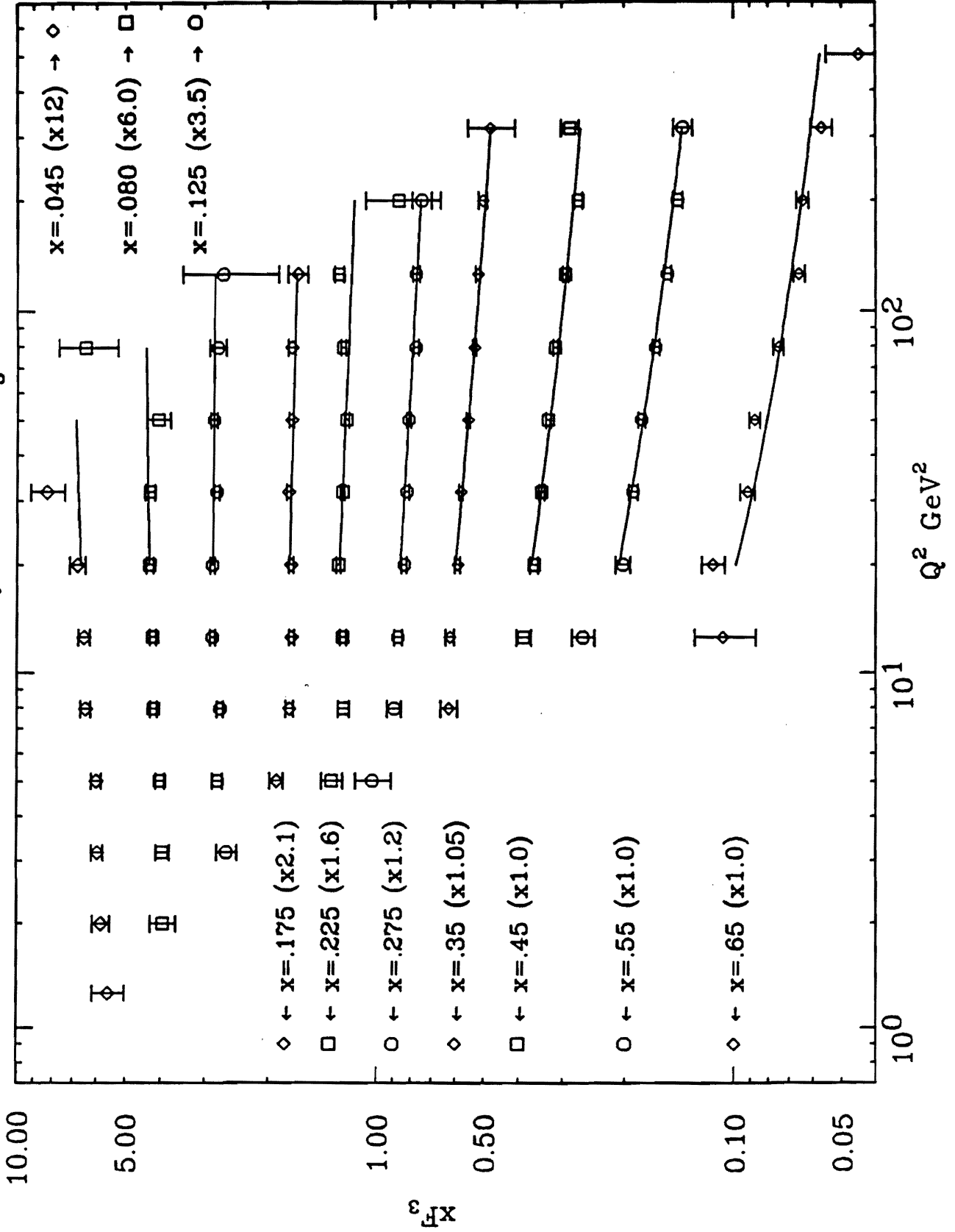
Figure 2: The xF_3 data and the best fit. Cuts of $Q^2 > 15 \text{ GeV}^2$ and $x < 0.7$ were applied for a next-to-leading order fit including target mass corrections.

Figure 3: The slopes of xF_3 ($= \frac{d \ln xF_3}{d \ln Q^2}$) for the CCFR data are shown in circles. The curve is a prediction from perturbative QCD with target mass correction. The slopes for F_2 (squares) in the region $x > 0.4$ are also shown (with x values shifted by +2% for clarity).

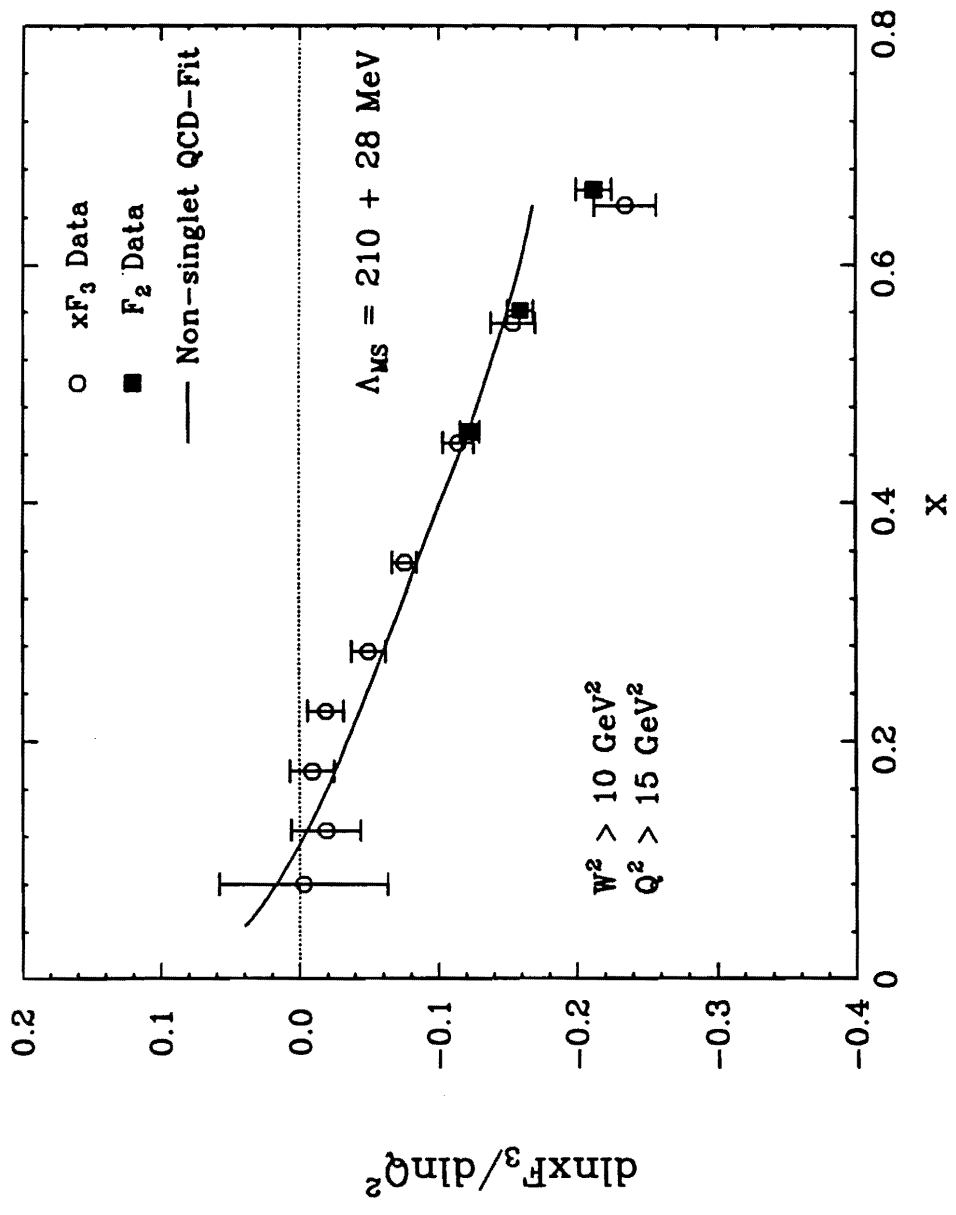
Figure 4: The slopes of F_2 ($= \frac{d \ln F_2}{d \ln Q^2}$) for the CCFR data are shown (squares). The curve is a prediction from perturbative QCD



CCFR: NLO QCD fits to xF_3



CCFR: Non-Singlet Slopes



CCFR: Singlet Slopes

